Electronic supporting information

Photoactivated cell-killing involving a low molecular weight, donor-acceptor diphenylacetylene

David R. Chisholm,[1] Rebecca Lamb,[2] Tommy Pallett,[1,3] Claire Holden,[1,2] Valerie Affleck,[4] Joanne Marrison,[5] Peter O'Toole,[5] Peter D. Ashton,[5] Katherine Newling,[5] Andreas Steffen,[6] Amanda K. Nelson,[6] Christoph Mahler,[6] Roy Valentine,[7] Thomas S. Blacker,[8] Angus J. Bain,[8] John Girkin,[3,*] Todd B. Marder,[6,*] Andrew Whiting[1,*] and Carrie A. Ambler[2,*]

Affiliations:

1 Department of Chemistry, Durham University, Science Laboratories, South Road, Durham, DH1 3LE, UK
2 Department of Biosciences, Durham University, South Road, Durham, DH1 3LE, UK
3 Biophysical Sciences Institute, Department of Physics, Durham University, South Road, Durham, DH1 3LE, UK
4 LightOx Limited, Wynyard Park House, Wynyard Avenue, Wynyard, Billingham, TS22 5TB, UK
5 Bioscience Technology Facility, Department of Biology, University of York, York, YO10 5DD, UK
6 Institut für Anorganische Chemie, Julius-Maximilians-Universität Würzburg, Am Hubland, 97074 Würzburg, Germany
7 High Force Research Ltd., Bowburn North Industrial Estate, Bowburn, Durham, DH6 5PF, UK.
8. Department of Physics & Astronomy, University College London, Gower Street, London, WC1E 6BT, UK

* Co-corresponding authors

Email: c.a.ambler@durham.ac.uk, andy.whiting@durham.ac.uk, j.m.girkin@durham.ac.uk, todd.marder@uni-wuerzburg.de

Table of contents

1. ^{1}H and ^{13}C NMR spectra

4-Iodobenzenediazonium tetrafluoroborate, 1

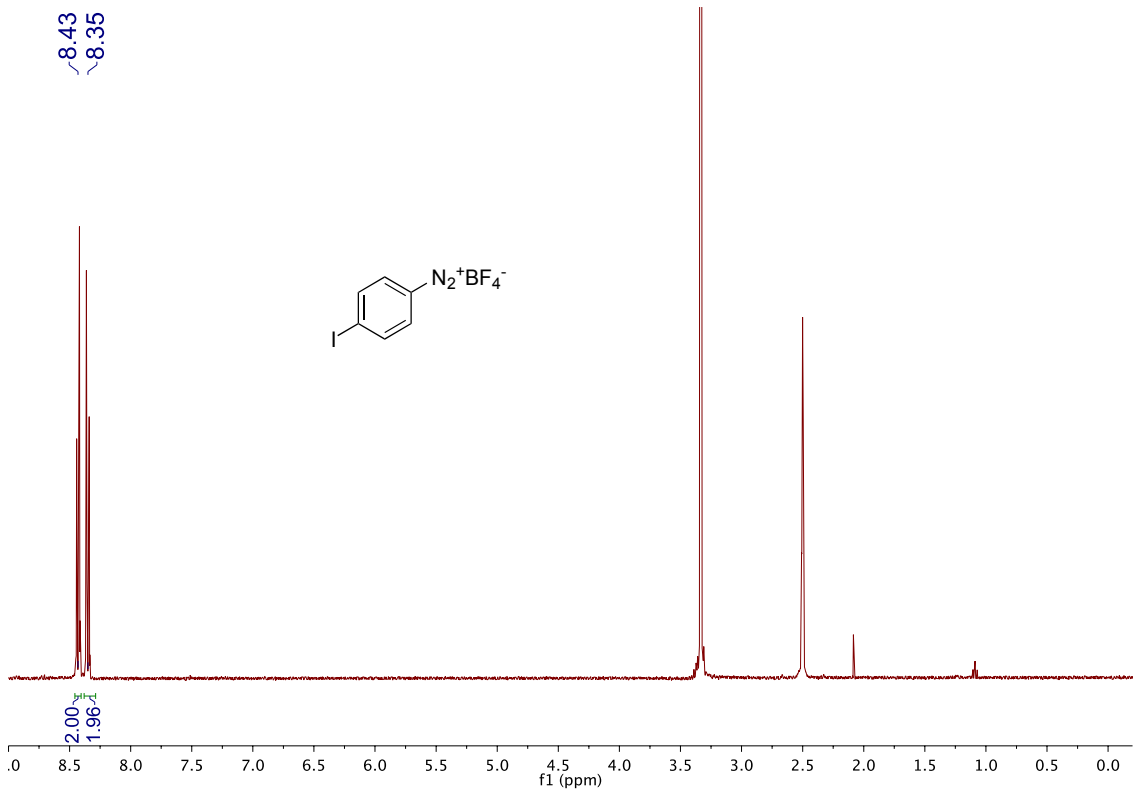

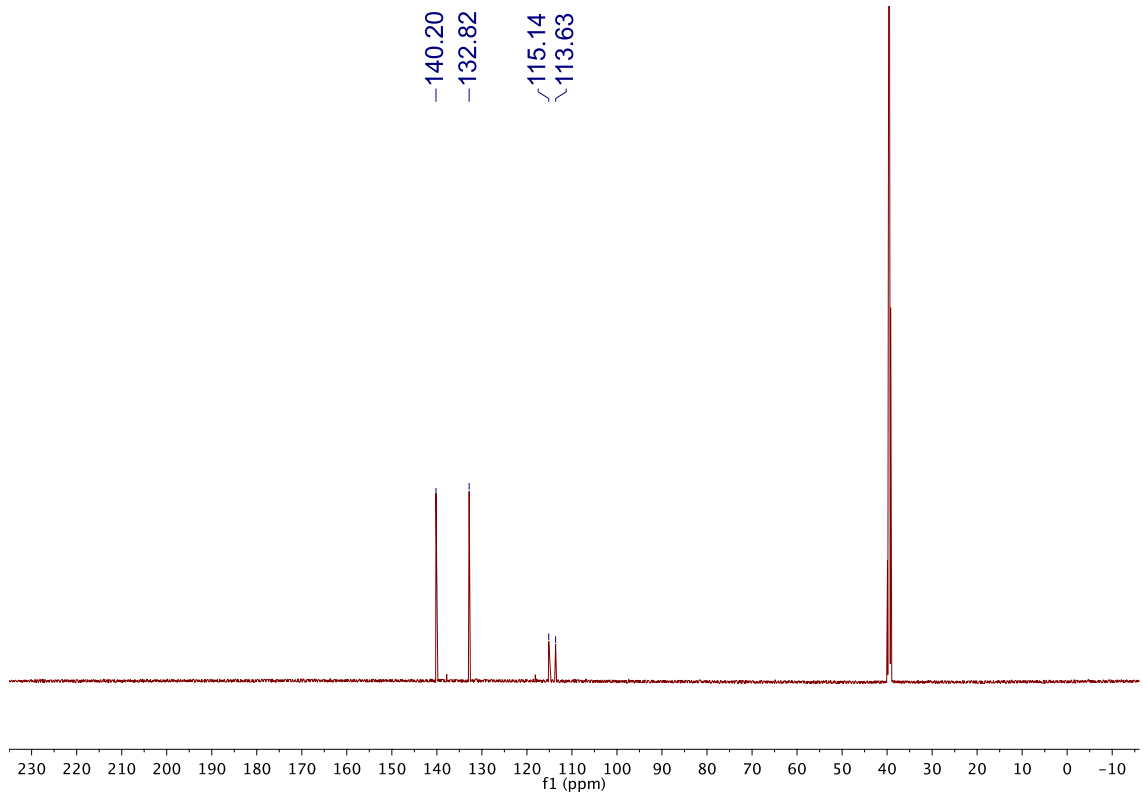

Methyl (2*E*)-3-(4-iodophenyl)prop-2-enoate, 2

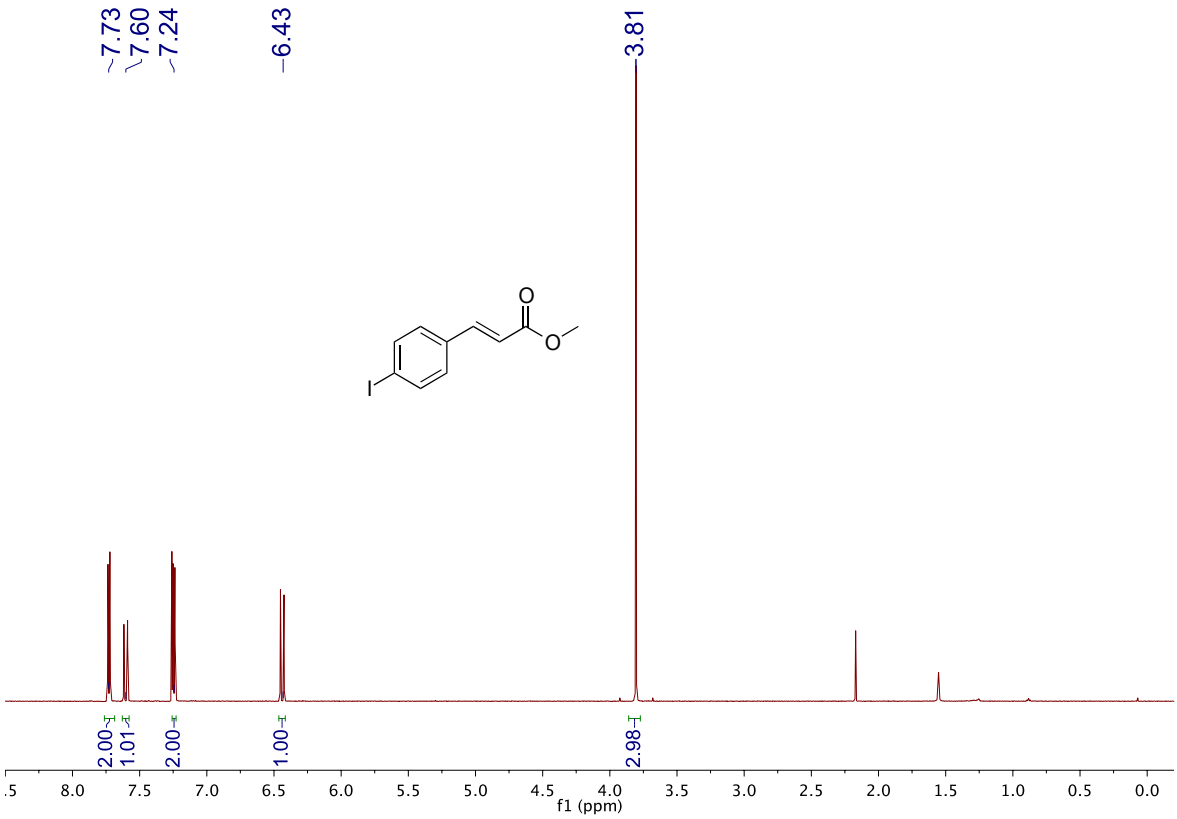

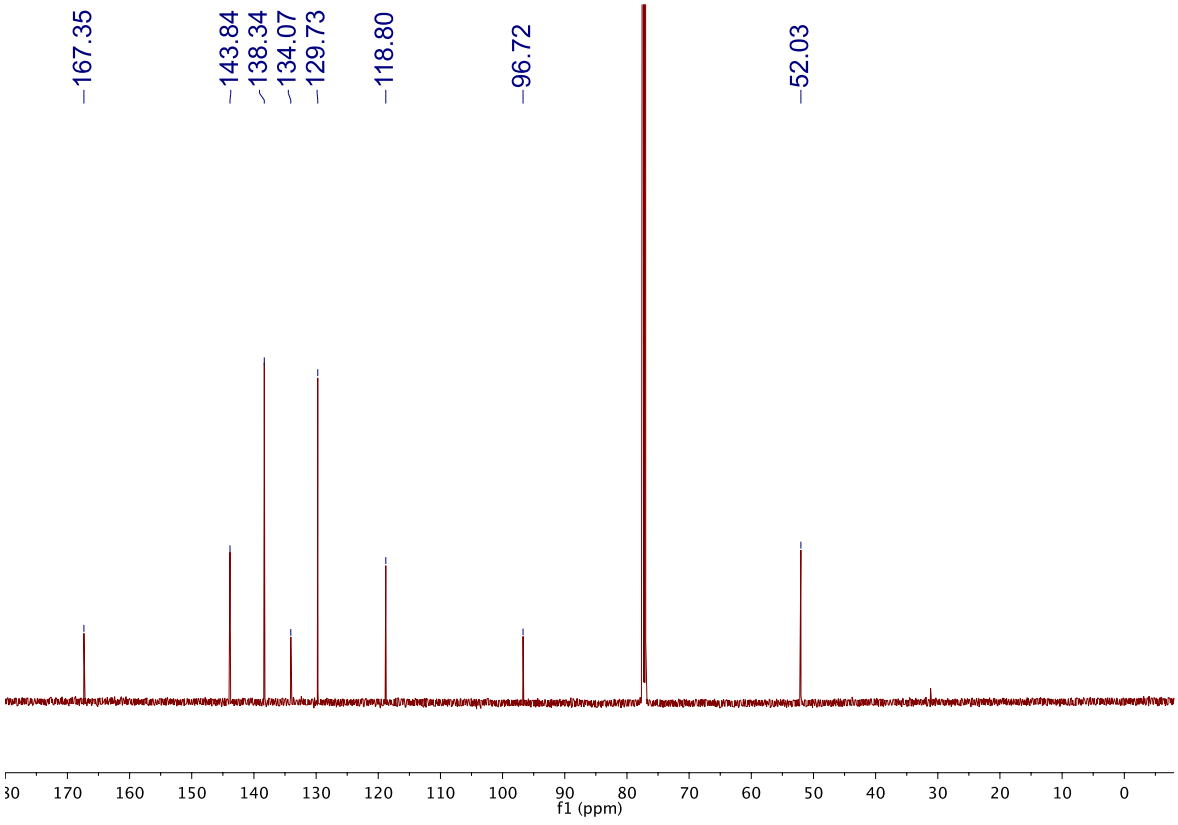

Methyl (2*E*)-3-4-[2-(trimethylsilyl)ethynyl]phenylprop-2-enoate, 3

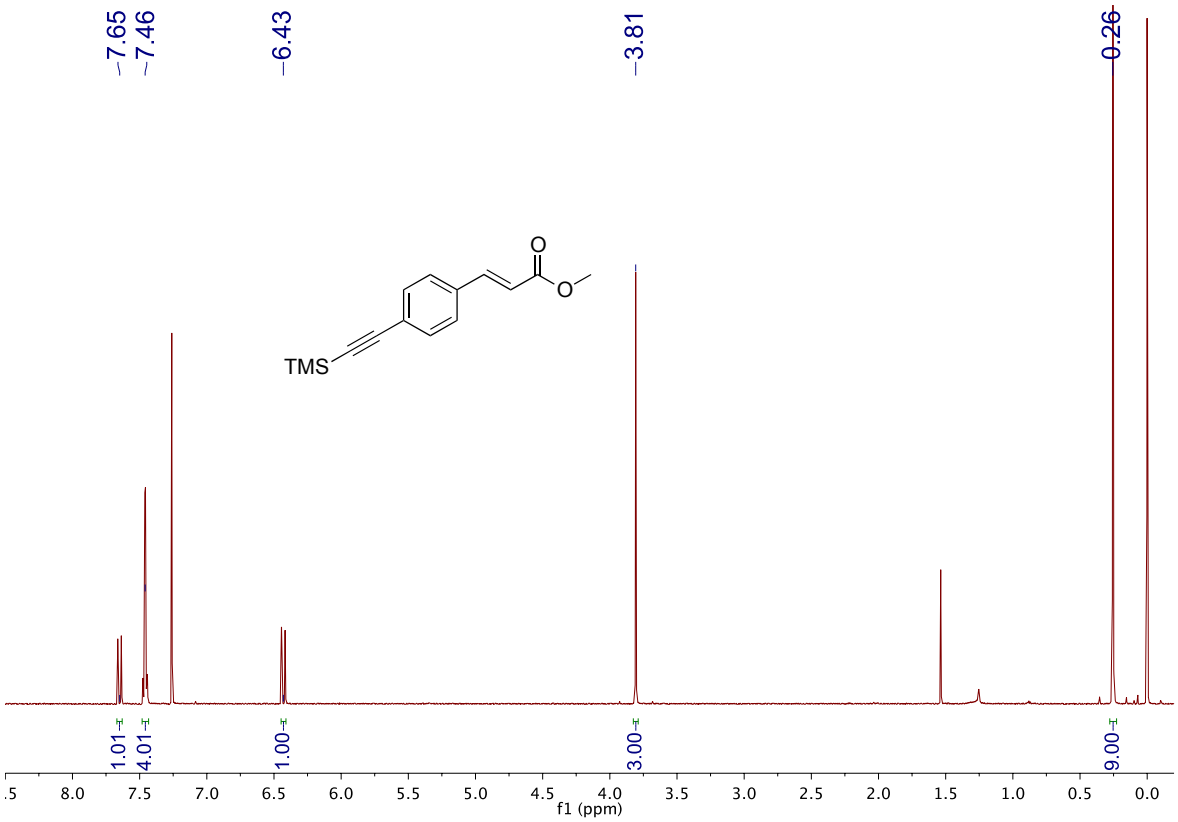

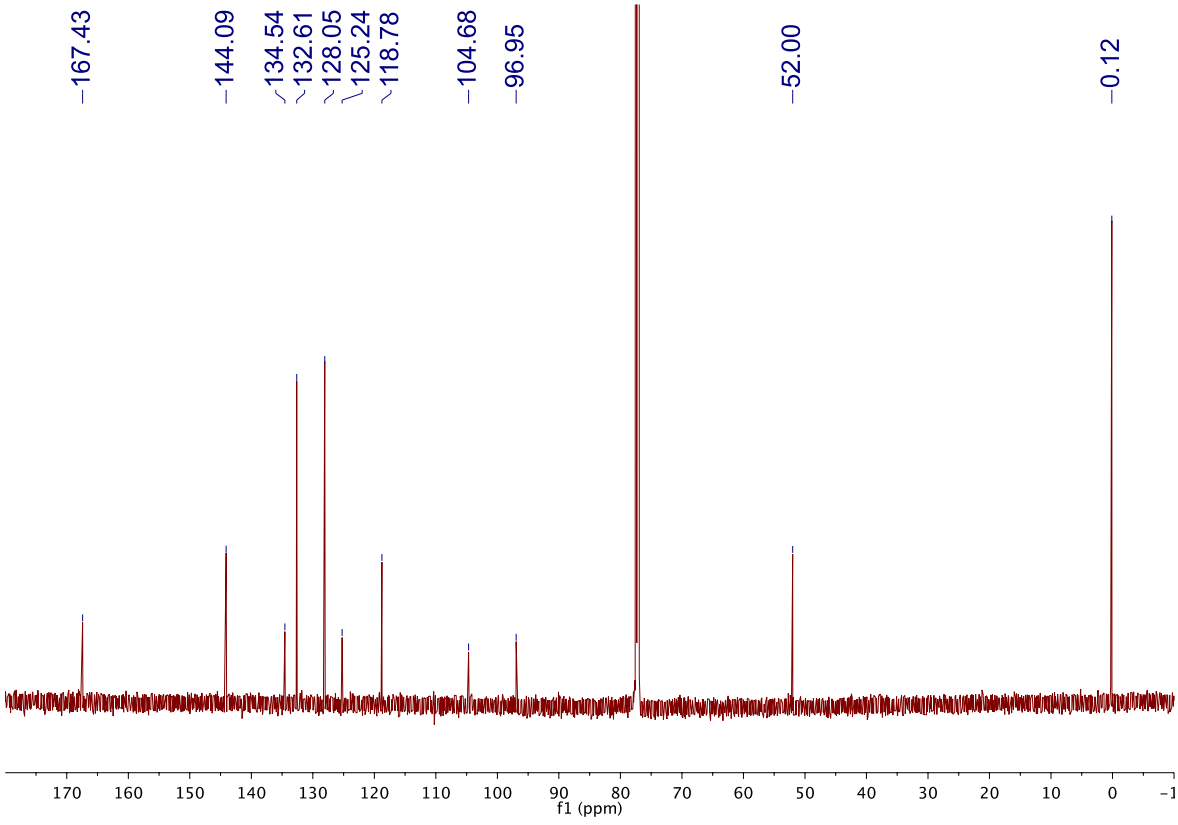

Methyl (2*E*)-3-(4-ethynylphenyl)prop-2-enoate, 4

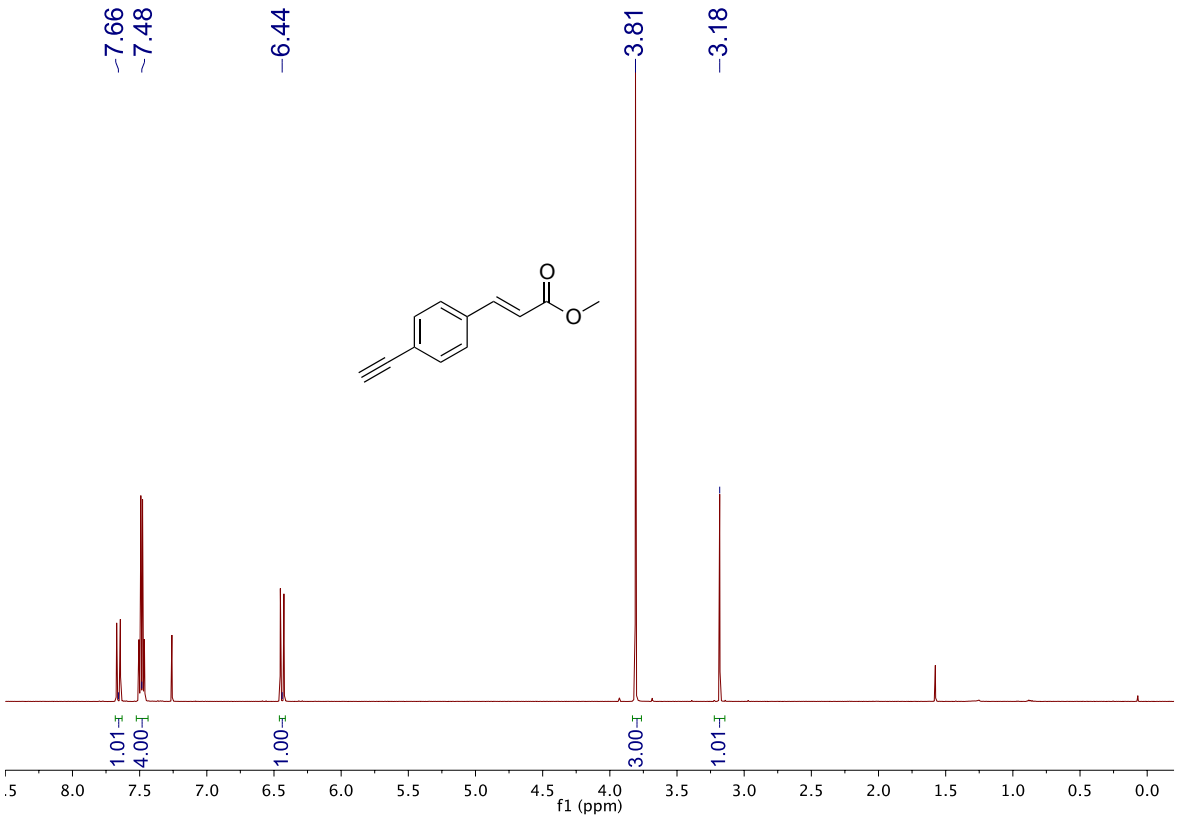
7.66
7.48
6.44
3.81
3.18
1.01
4.00
1.00
3.00
1.01
f1 (ppm)

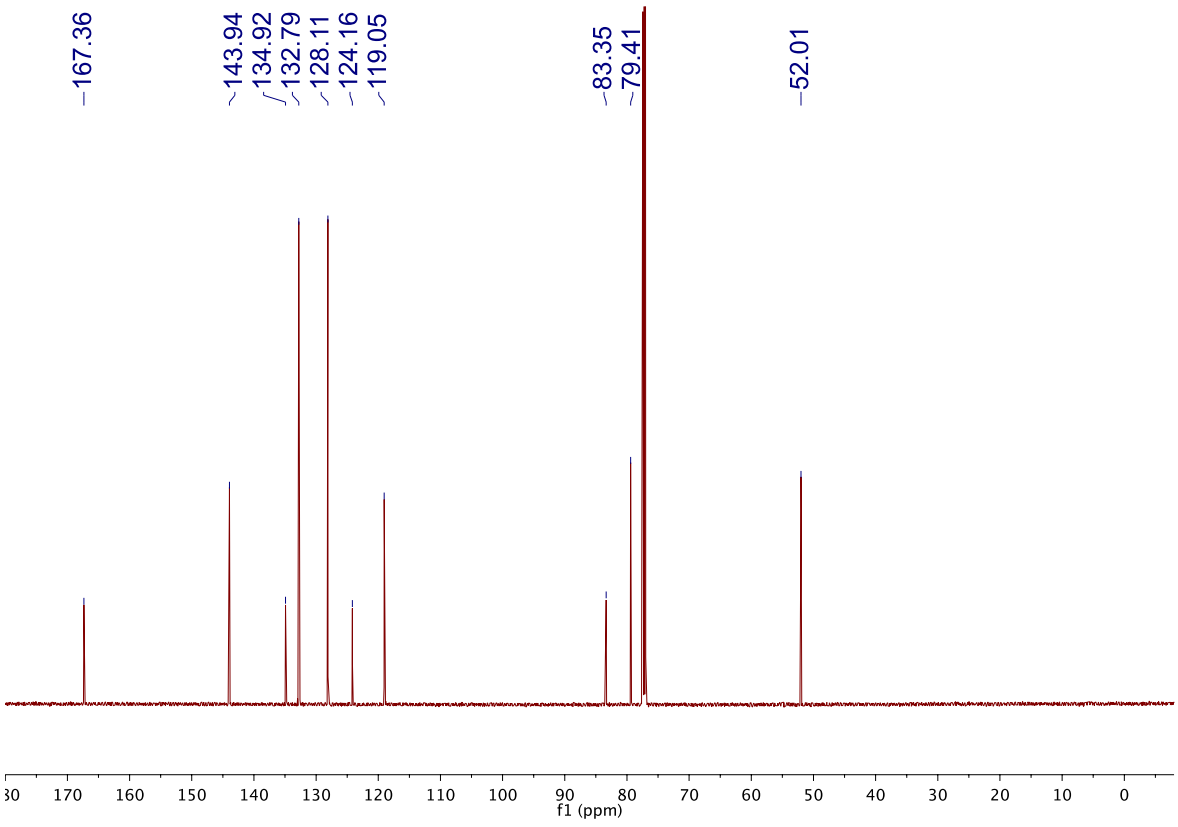
167.36
143.94
134.92
132.79
128.11
124.16
119.05
83.35
79.41
52.01
f1 (ppm)

(2*E*)-3-(4-{2-[4,4-Dimethyl-1-(propan-2-yl)-1,2,3,4-tetrahydroquinolin-6-yl]-ethynyl}phenyl)prop-2-enoic acid, DC324

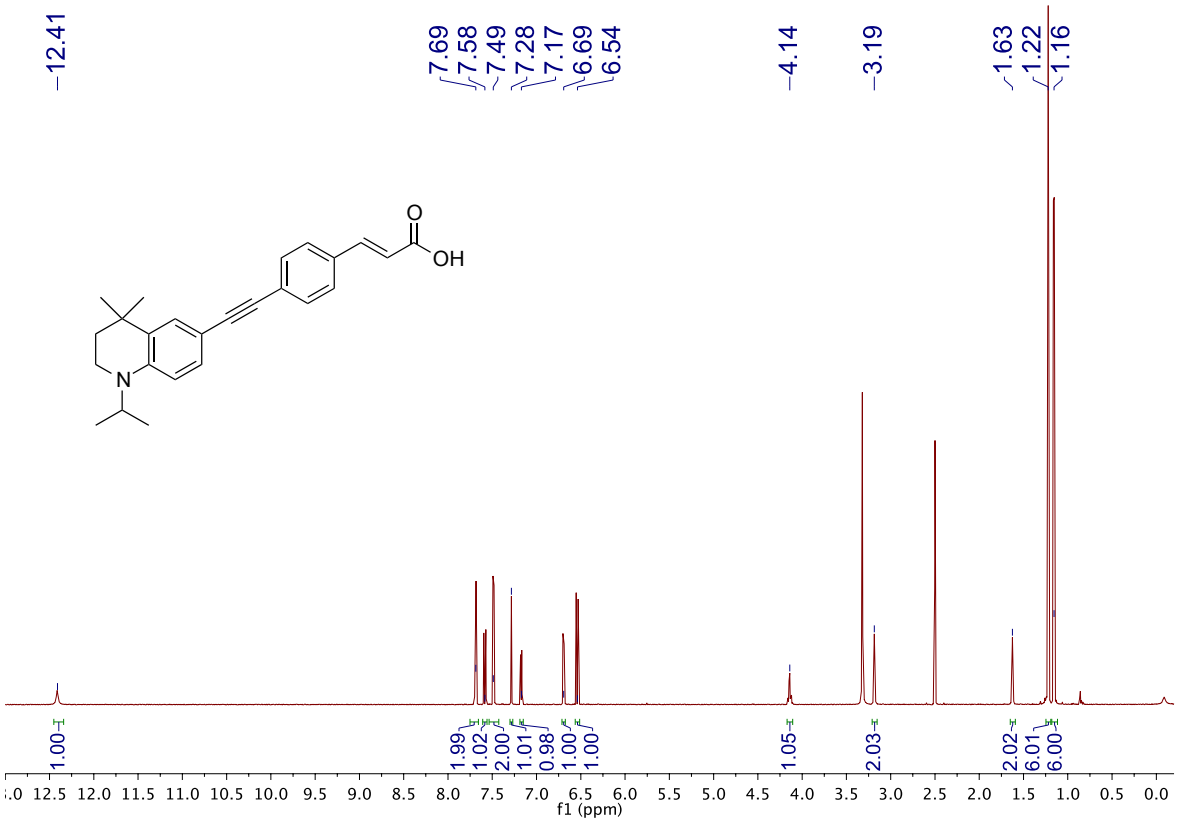

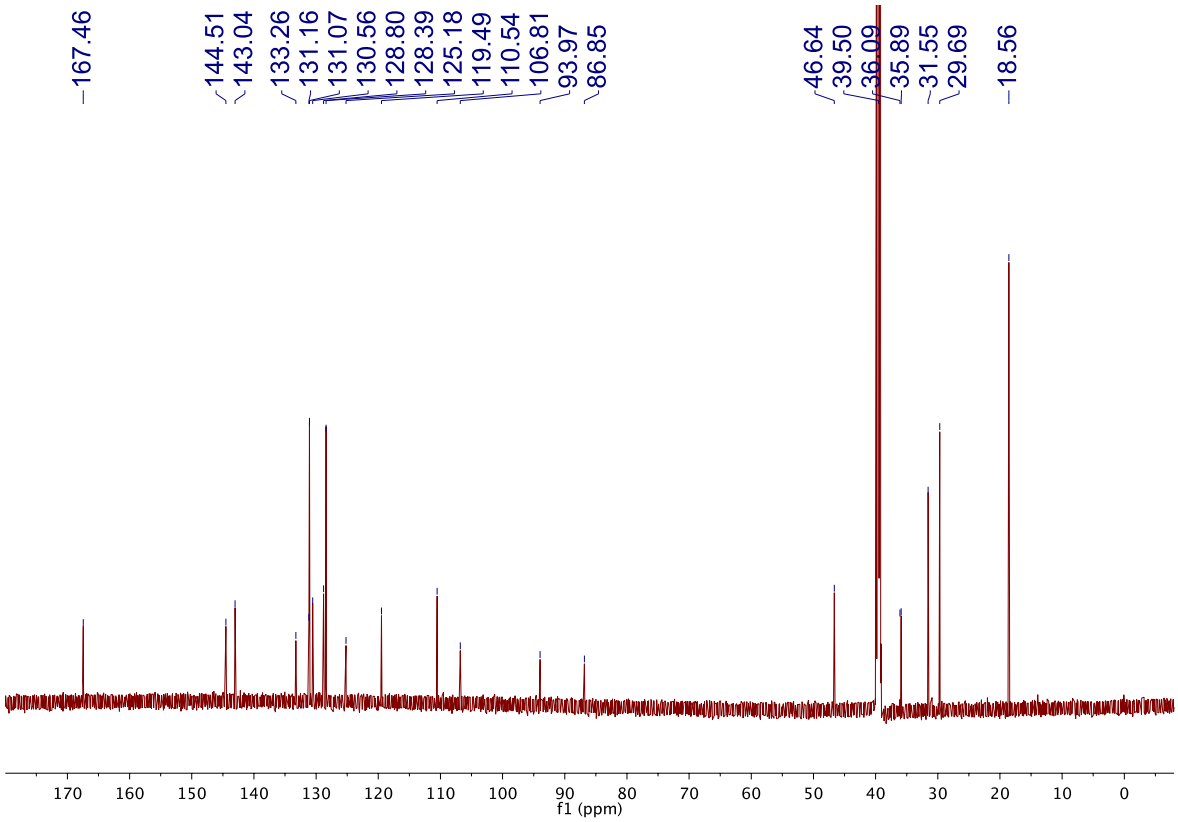

2. ROS detection experiments

2.1 $^1O_2$ detection

Solutions of DC324 in EtOH, CH_2Cl_2, CD_2Cl_2, toluene and D_8-toluene were prepared and saturated with molecular oxygen by bubbling pure O_2 through the solutions for a minimum of 10 minutes. The samples were placed in the Edinburgh Instruments FLSP920 spectrometer equipped with a nitrogen-cooled NIR PMT detector located after the first monochromator covering an emission wavelength range between 500-1400 nm with ca. 1000 dark cps. During illumination with wavelengths corresponding to the two absorption maxima in the respective solvent, the phosphorescence of $^1O_2$ at 1270 nm was investigated. The known $^1O_2$-producing standard $[Ru(bpy)_3](PF_6)_2$ was used as a reference. We have tested several solutions with an optical density (OD) of DC324 of 0.2-0.8. $^1O_2$ was not detected in these experiments.

2.2 Hydroxyl radical detection

Solutions of DC324 in EtOH/H_2O (3 mL / 0.5 mL) were prepared and Methylene Blue, which is known to degrade in the presence of hydroxyl radicals, was added. The solutions were saturated with molecular oxygen by bubbling with pure O_2 for a minimum of 10 minutes, and irradiated separately with 365 nm and 405 nm light for 30 minutes. The absorption spectra were recorded every 10 minutes to monitor changes in the Methylene Blue absorption. We tested a range of relative concentrations of DC324 and Methylene Blue, i.e. with OD(DC324) = 0.5-0.8 and OD(Methylene Blue) = 0.2-0.5. Hydroxyl radical was not detected in these experiments.

2.3 Peroxyl radical detection

DC324 was dissolved in toluene, D_8-toluene or EtOH to give an optical density of 0.2-0.8, and Rhodamine 6G (Rh6G) was added (OD = 0.2). The solutions were saturated with molecular oxygen by bubbling with pure O_2 for a minimum of 10 minutes, and irradiated at the lowest energy absorption maximum in the respective solvent for 30 minutes. The quenching of the absorption and of the fluorescence of Rh6G due to oxidation by peroxyl radicals was monitored every 10 minutes. The same procedure was applied also to solutions with added H_2O (50-500 µl). Peroxyl radical was not detected in these experiments.

2.4 Hydrogen peroxide detection

Solutions containing DC324 (OD = 0.2-0.8) and luminol (OD = 0.2-0.8) in EtOH/H_2O (3 mL / 0.5 mL) were prepared, saturated with molecular oxygen by bubbling with pure O_2 for a minimum of 10 minutes and irradiated for 5-30 minutes with 375 nm or 405 nm light. Upon addition of a few crystals of $CoCl_2$ as catalyst, the chemiluminescence of the oxidation process of luminol initiated by H_2O_2 was monitored. H_2O_2 was not detected in these experiments.

3. Cellular experiments and imaging

3.1 Optical power measurements

The optical power delivered to the sample was measured using a Thorlabs PM100A meter with a S120VC UV enhanced detector. This was then placed under microscope objective to measure the optical power delivered to the sample either in the Zeiss 880 or Zeiss Axio Vert A1. In the case of the confocal measurement the meter calibration was set at 405 nm and for the fluorescence system to 370 nm, the peak of the spectral emission after the DAPI filter. To measure the confocal power the beam was parked in the centre of the field and the photodiode head positioned to ensure all of the light was hitting the detector. The power was then measured and calibrated against the power setting on the Zeiss control software. This exercise was repeated before all measurements. This determines the power delivered to each pixel and, by multiplying by the pixel dwell time, the energy delivered to each pixel per scan. The energy delivered per exposure can then be determined knowing the overall scan speed and the time of exposure. The laser power was measured to be 85 +/- 5 µW at the 5% power setting used for all laser irradiation treatments.

For the epi-illumination system (Zeiss Axio Vert) an area delimiting mark was placed into the optical system and a uniform fluorescent sea placed under the system. The fluorescence was then imaged and the area being illuminated, through the mask, determined using ImageJ where the images had been previously spatially calibrated using a scaled grating. The measured region was 0.54 × 0.35 ± .025 mm.

The photodiode detector was then placed under the objective to collect all of the light delivered to the sample through the mask. The average power was determined to be 1.32 ± 0.3 mW giving a power density of 0.7 W/cm^2. The total energy delivered was then determined based upon the exposure time to give an energy flux in J/cm^2.

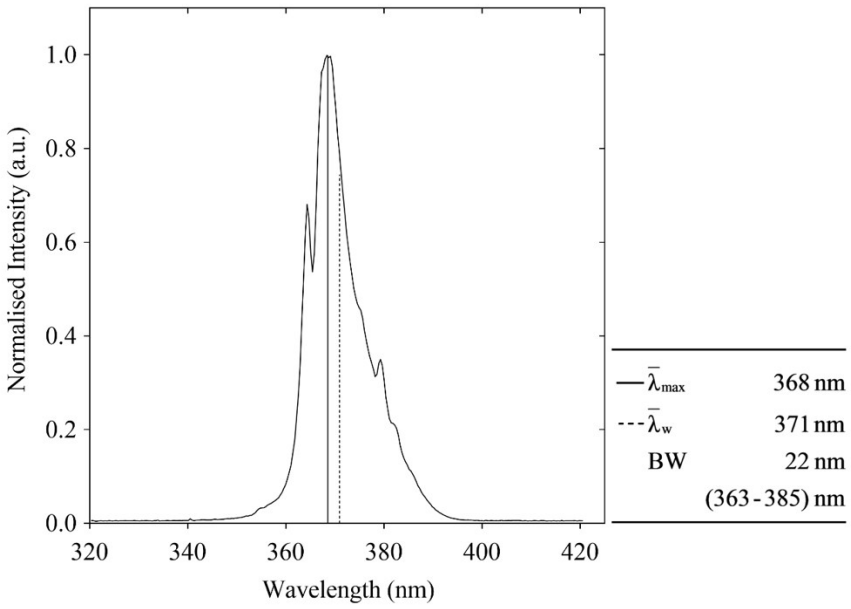

Figure S1: The light spectrum of the DAPI excitation-filtered mercury bulb over a restricted domain of 320-420 nm. Values outside of this range were deemed vanishingly small. Relevant features of the spectrum are included to the right-hand side. $\bar{\lambda}_{max}$ = the average maximum wavelength (over repeated measurements); $\bar{\lambda}_{w}$ = the average weighted wavelength; BW = the bandwidth of the spectrum.

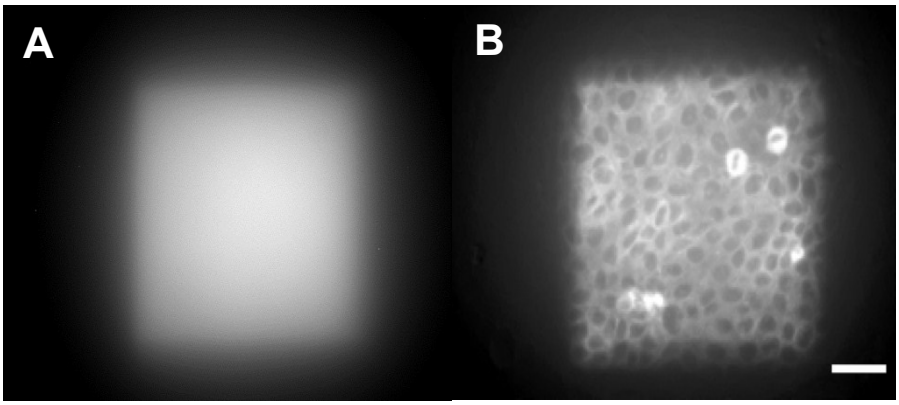

Figure S2: Irradiation zone using Axio Vert live imaging microscope. (A) The irradiation zone formed from focussing the DAPI-filtered mercury bulb in a blank well of a 6-well plastic tissue culture dish using a 10× EC Plan Neo-fluor objective. (B) The same irradiation zone illuminating DC324-treated HaCaT cells. The illumination boundaries are well defined by the DAPI-filtered light source bounded by an opaque adjustable filter. Scale bar equals 100 µm.

3.2 Lambda emission scan

Cells were prepared and treated as described previously. Compounds were excited using 405 nm laser light and imaged in the Zeiss 880 LSCM "lambda scan" mode with automated capture of emission wavelength and intensity at 5 nm steps over the range of 410-700 nm. Zeiss Zen Blue software was used to graph relative intensity measurements and the 'unmixing' function was used to examine different regions of interest (ROIs) in a single field of view.

3.3 Multiphoton imaging

Imaging was carried out using a Zeiss LSM 780 multiphoton microscope fitted with a pulsed Coherent Chameleon Ultra laser and Solent Scientific incubation chamber. Before irradiation with high laser powers, images were captured for each treatment using a Plan Apochromat 20x/0.8 objective, 0.6x digital zoom, 1% (11 mW after objective) 800 nm laser and emission was detected at 500-550 nm. The coordinates of these regions of interest were saved to the software's position list and used for irradiation and post-irradiation imaging. Regions of interest were then irradiated with between 10-22.5% in 2.5% increments (111-260 mW) 800 nm laser, using a Plan Apochromat 20x/0.8, 1x digital zoom, 6.3 msec pixel dwell time, 830 nm, 512 x 512 pixels and no averaging. After irradiation with high laser power the regions of interest were reimaged every 10 minutes over 22 hours using a Plan Apochromat 20x/0.8 objective, 0.6x digital zoom, 1% (11 mW) 800 nm laser and emission detected at 500-550 nm.

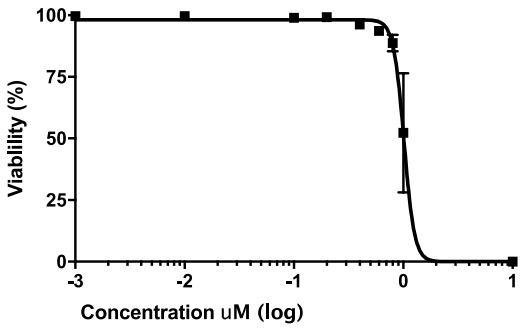

Figure S3: The average viable fraction of HT29 colorectal cancer cells 24 hours after an initial 60 seconds UV-exposure, as a function of the concentration of DC324 administered. A non-linear regression curve is fitted to the data (experimental replicates, n = 3; R^2 = 0.99; EC_{50} = 1.015 µM).

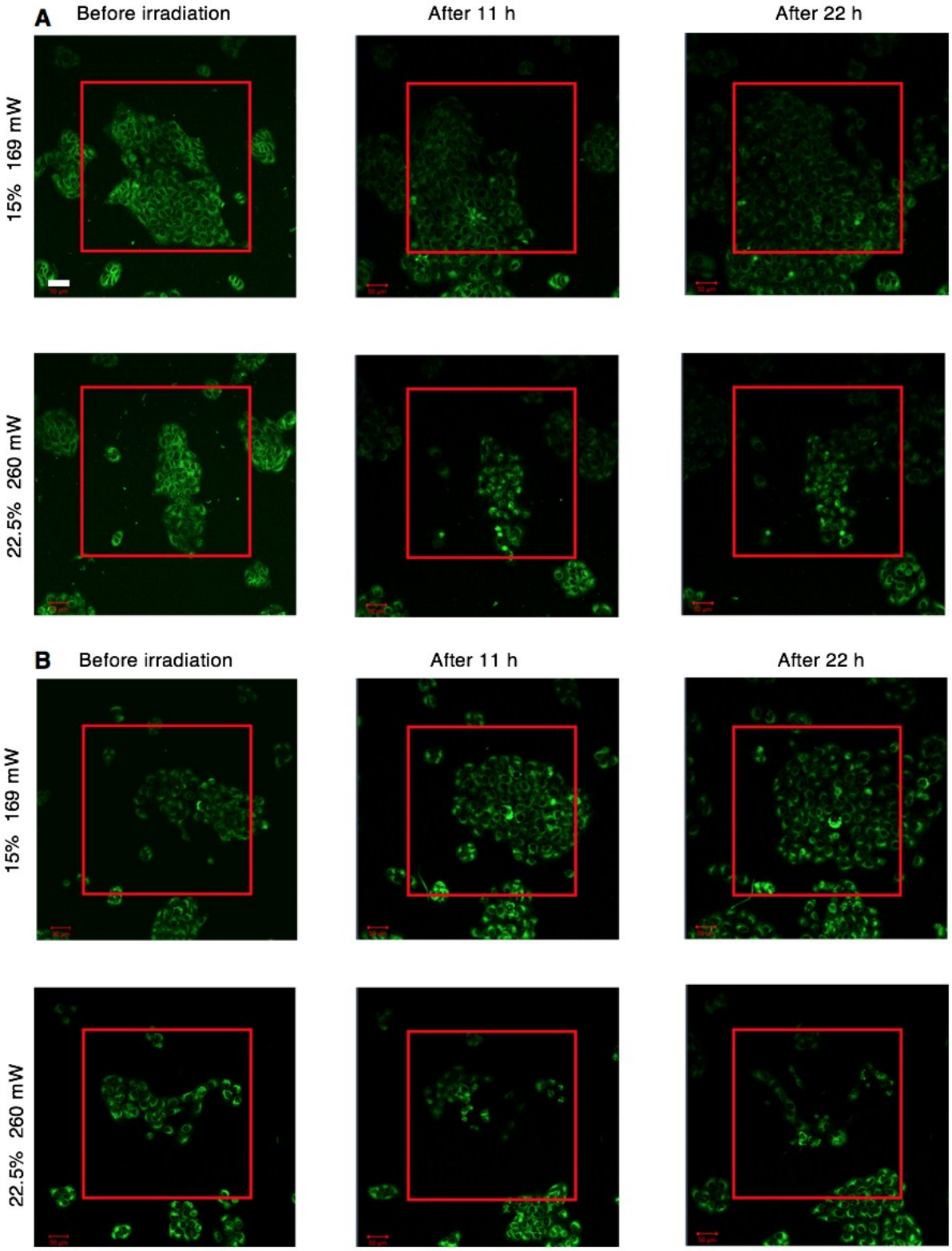

Figure S4: Two photon excited fluorescence images of DC324 and DC473. Cells were treated with 10 μM DC324 (A) or DC473 (B). Images shown are either pre-irradiation or 11 hours and 22 hours post-irradiation at 169 mW or 260 mW laser power at 800 nm. Cell growth was arrested post-irradiation as seen by loss of dynamic cell growth in the irradiated zone (260 mW) after both 11 and 22 hours, but cells irradiated at 169 mW laser power were mostly unaffected. Red box shows region of irradiation. Note that two-photon absorption is proportional to the square of the intensity (I^2).

3.4 Two-photon absorption measurements

Two-photon absorption spectra were measured using the method of Xu and Webb.[1] Briefly, the time-averaged fluorescence intensity of the two compounds were compared with that of a reference standard with a well characterised two photon absorption spectrum (rhodamine B in methanol, data obtained online from Zipfel Lab, Cornell University). Solutions of DC324 and DC473 in toluene (of the order of 10^{-4} M) were held in 50 µl quartz optical cuvettes. Two-photon fluorescence was excited by the output of a Ti:Sapphire laser tuned between 730 and 870 nm (Coherent Mira 900F) and fluorescence was registered by a multichannel plate PMT (Hamamatsu). Concentrations of each solution were determined by measuring their absorbance with a xenon white light source, USB spectrometer and the known extinction coefficients.[2,3] Spectral detection efficiencies were corrected for the transmission efficiency of the emission filters, the spectral response of the detector provided by the manufacturer and the emission spectra of the compounds (obtained from the literature for rhodamine[4]). Refractive indices of the solvents were obtained from the literature.[5,6] Error bars on the graphs reflect the SEM from three repeats.

3.5 RNA sequencing experiments

mRNAs were sequenced to determine what gene products were transcribed in cells undergoing experimental conditions. Lists of differentially expressed genes from RNAseq were determined from experimental cells that were treated with 1 μM DC473 and then irradiated and compared with the expressed genes from control cells (non-irradiated cells treated with 1 μM DC473, cells treated with 0.1% DMSO, or irradiated cells treated with 0.1% DMSO).

To analyse the key cellular and biological processes affected, these lists of differentially expressed genes were compared to those in the internationally curated collection of gene sets, which have known biological roles and functions, called the Gene Ontology (GO) knowledgebase (curated by The Gene Ontology Consortium). The GO knowledgebase is the world's largest source of information on the functions of genes and sets of genes. Using online software provided by the Broad Institute, lists of genes from the RNAseq analysis was compared to the lists of genes in the GO collection. Only the ten gene sets in the GO collection with that highest overlap with each gene set were included in the table below[7].

Please note that analysis of these RNA samples indicated that, among other effects, genetic responses resulting from the presence of oxygen species were detected only in irradiated cells treated with DC473 in comparison to controls.

DC473 (not irradiated) vs. DC473 (irradiated)	# Genes in Set (K)	# Genes in Overlap (k)	p-value	FDR q-value
GO_CELLULAR_RESPONSE_TO_ORGANIC_SUBSTANCE	1848	63	5.51E-27	3.26E-23
GO_RESPONSE_TO_ENDOGENOUS_STIMULUS	1450	53	4.70E-24	1.39E-20
GO_RESPONSE_TO_OXYGEN_CONTAINING_COMPOUND	1381	51	2.38E-23	4.69E-20
GO_REGULATION_OF_CELL_DEATH	1472	50	2.46E-21	3.63E-18
GO_RESPONSE_TO_ABIOTIC_STIMULUS	1024	41	4.04E-20	4.78E-17
GO_RESPONSE_TO_NITROGEN_COMPOUND	859	37	2.88E-19	2.61E-16
GO_TISSUE_DEVELOPMENT	1518	48	3.08E-19	2.61E-16
GO_POSITIVE_REGULATION_OF_GENE_EXPRESSION	1733	51	4.29E-19	3.17E-16
GO_CELLULAR_RESPONSE_TO_ENDOGENOUS_STIMULUS	1008	38	7.74E-18	4.93E-15
GO_CELL_CYCLE	1316	43	8.33E-18	4.93E-15
DMSO (irradiated) vs. DC473 (irradiated)	# Genes in Set (K)	# Genes in Overlap (k)	p-value	FDR q-value
GO_POSITIVE_REGULATION_OF_GENE_EXPRESSION	1733	100	1.91E-37	1.13E-33
GO_REGULATION_OF_TRANSCRIPTION_FROM_RNA_POLYMERASE_II_PROMOTER	1784	97	3.34E-34	9.87E-31
GO_REGULATION_OF_INTRACELLULAR_SIGNAL_TRANSDUCTION	1656	93	7.46E-34	1.26E-30
GO_POSITIVE_REGULATION_OF_BIOSYNTHETIC_PROCESS	1805	97	8.53E-34	1.26E-30
GO_REGULATION_OF_CELL_DEATH	1472	87	2.90E-33	3.43E-30
GO_CELLULAR_RESPONSE_TO_ORGANIC_SUBSTANCE	1848	96	2.80E-32	2.77E-29
GO_TISSUE_DEVELOPMENT	1518	86	1.50E-31	1.27E-28
GO_NEGATIVE_REGULATION_OF_GENE_EXPRESSION	1493	85	2.47E-31	1.83E-28
GO_NEGATIVE_REGULATION_OF_RESPONSE_TO_STIMULUS	1360	81	3.46E-31	2.27E-28
GO_RESPONSE_TO_OXYGEN_CONTAINING_COMPOUND	1381	80	5.43E-30	3.21E-27
DMSO (non-irradiated) vs. DMSO (irradiated)	# Genes in Set (K)	# Genes in Overlap (k)	p-value	FDR q-value
GO_TISSUE_DEVELOPMENT	1518	76	1.01E-32	5.95E-29
GO_REGULATION_OF_CELL_PROLIFERATION	1496	75	2.52E-32	7.45E-29
GO_REGULATION_OF_CELL_DIFFERENTIATION	1492	74	1.37E-31	2.70E-28
GO_RESPONSE_TO_EXTERNAL_STIMULUS	1821	80	1.34E-30	1.98E-27
GO_NEGATIVE_REGULATION_OF_MULTICELLULAR_ORGANISMAL_PROCESS	983	58	1.33E-28	1.57E-25
GO_CELLULAR_RESPONSE_TO_ORGANIC_SUBSTANCE	1848	77	5.89E-28	5.80E-25
GO_REGULATION_OF_MULTICELLULAR_ORGANISMAL_DEVELOPMENT	1672	73	1.01E-27	8.53E-25
GO_CELL_MOTILITY	835	52	8.75E-27	6.47E-24
GO_LOCOMOTION	1114	59	1.18E-26	7.78E-24
GO_POSITIVE_REGULATION_OF_RESPONSE_TO_STIMULUS	1929	76	4.52E-26	2.67E-23

Table S1: Gene ontology (GO) analysis. The statistical significance of the overlap between genes in a pathway and the list of differently expressed genes was determined by Fisher's exact test including both standard p-value and Benjamini-Hochberg false discovery rate (FDR) q-value.

4. X-ray Crystallography

Single-crystal diffraction experiments were conducted on a Bruker APEX-II CCD diffractometer. Crystals were cooled using Cryostream (Oxford Cryosystems) open-flow N_2 cryostats. The structures were solved within Olex2 by direct methods and refined by full-matrix least squares against F^2 of all data, using SHELXTL software.[8–11] All non-hydrogen atoms were refined anisotropically. Hydrogen atom positions were calculated geometrically and refined using the riding model. CCDC (1854354) contains the supplementary crystallographic data for this paper.

4.1 Methyl (2*E*)-3-(4-iodophenyl)prop-2-enoate, 2

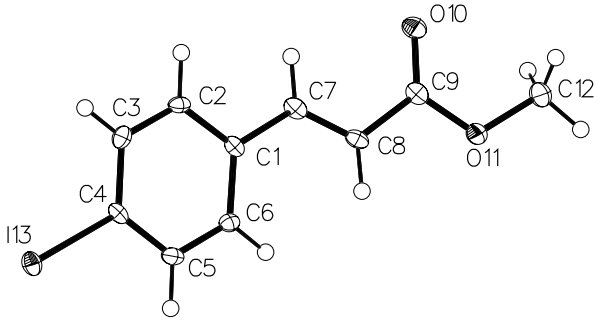

Figure S5: X-ray molecular structure of compound **2**. Anisotropic displacement ellipsoids are drawn at the 50% probability level. Selected bond distances (Å): C(7)-C(8) 1.341, C(9)-O(10) 1.210, C(9)-O(11) 1.330, C(1)-C(7) 1.458, C(4)-I(13) 2.088.

Empirical formula	$C_{10}H_9IO_2$
Formula weight	288.07
Temperature/K	120
Crystal system	orthorhombic
Space group	$Pbc2_1$
a/Å	6.9818(3)
b/Å	6.0984(3)
c/Å	23.2221(11)
α/°	90
β/°	90
γ/°	90
Volume/Å^3	988.75(8)
Z	4
ρ_{calc} g/cm^3	1.935
μ/mm^{-1}	3.202
F(000)	552
Crystal size/mm^3	0.245 × 0.139 × 0.04
Radiation	MoKα (λ = 0.71073)
2θ range for data collection/°	5.836 to 70.96
Index ranges	-11 ≤ h ≤ 10, -9 ≤ k ≤ 9, -36 ≤ l ≤ 37
Reflections collected	24525
Independent reflections	4256 [R_{int} = 0.0559, R_{sigma} = 0.0578]
Data/restraints/parameters	4256/1/119
Goodness-of-fit on F^2	1.057
Final R indexes [I>=2σ (I)]	R_1 = 0.0397, wR_2 = 0.0579
Final R indexes [all data]	R_1 = 0.0706, wR_2 = 0.0634
Largest diff. peak/hole / e Å^{-3}	1.43/-2.87
Flack parameter	0.014(14)

Table S2: Crystallographic data for compound **2**. CCDC (1854354) contains the full supplementary crystallographic data for this paper. The data can be obtained free of charge from The Cambridge Crystallographic Data Centre via www.ccdc.cam.ac.uk/getstructures.

5. References

1 C. Xu and W. W. Webb, *J. Opt. Soc. Am. B*, 1996, **13**, 481–491.

2 J. Gala De Pablo, D. R. Chisholm, A. Steffen, A. K. Nelson, C. Mahler, T. B. Marder, S. A. Peyman, J. M. Girkin, C. A. Ambler, A. Whiting and S. D. Evans, *Analyst*, 2018, **143**, 6113–6120.

3 M. Taniguchi and J. S. Lindsey, *Photochem. Photobiol.*, 2018, **94**, 290–327.

4 A. S. Kristoffersen, S. R. Erga, B. Hamre and Ø. Frette, *J. Fluoresc.*, 2014, **24**, 1015–1024.

5 H. El-Kashef, *Phys. B*, 2000, **279**, 295–301.

6 S. Kedenburg, M. Vieweg, T. Gissibl and H. Giessen, *Opt. Mater. Express*, 2012, **2**, 1588–1611.

7 A. Subramanian, P. Tamayo, V. K. Mootha, S. Mukherjee, B. L. Ebert, M. A. Gillette, A. Paulovich, S. L. Pomeroy, T. R. Golub, E. S. Lander and J. P. Mesirov, *Proc. Natl. Acad. Sci. USA*, 2005, **102**, 15545–15550.

8 O. V. Dolomanov, L. J. Bourhis, R. J. Gildea, J. A. K. Howard and H. Puschmann, *J. Appl. Cryst.*, 2009, **42**, 339–341.

9 G. M. Sheldrick, *Acta Cryst.*, 2015, **C71**, 3–8.

10 G. M. Sheldrick, *Acta Cryst.*, 2015, **A71**, 3–8.

11 APEX2, SAINT and SADABS, *Bruker AXS Inc., Madison, Wisconsin, USA*.